

THE SPATIOTEMPORAL DYNAMICS OF AFRICAN CASSAVA MOSAIC DISEASE

Z. LAWRENCE AND D. I. WALLACE

Department of Mathematics

Dartmouth College, HB 6188

Hanover, NH, 05755, USA

E-mail: Dorothy.Wallace@Dartmouth.edu

African Cassava Mosaic Disease, a vector-borne plant disease, causes massive food shortages throughout sub-Saharan Africa. A system of ordinary differential equations is used to find the equilibrium values of the whitefly vector and the cassava plants it affects. The temporal ODE system is modified to incorporate the spatial dynamic. The resulting system of advection-diffusion equations is analyzed using finite differencing in MATLAB to assess the spatiotemporal spread of ACMD. The partial differential equations system is systematically altered and solutions are assessed in terms of the relative cassava yield they predict. Simulations include parameter sensitivity analysis, spatial modifications, analysis of the impact of a source term, and initial condition variance. Results are compared with field data. Practical implications of these simulations for controlling ACMD are explored. Data suggests that the use of windbreaks and ACMD resistant strains of cassava will have the most beneficial impact on cassava yield.

1. Introduction

The average person in Africa eats about 80 kg of cassava per year [1] and total annual production is approximately 85 million tons, more than any other crop in the African continent [2]. A starchy, potato-like source of carbohydrates, cassava root is a versatile food source that can be prepared and consumed according to a variety of different methods. Cassava is a major part of the diets of many of the worlds citizens; the health and stability of this staple sub-Saharan African food crop is therefore of the utmost importance. Cassava production has been severely affected by a devastating virus known as the African Cassava Mosaic Disease (ACMD). First discovered in 1928, this virus is transmitted via the whitefly *Bemisia tabaci Gennadius* and can result in substantial losses to cassava harvests. [3] An affected plant has a chlorotic mosaic on infected leaves. Although the stem and roots of the cassava plant do not show symptoms of the

disease, chlorosis of the leaves interferes with photosynthesis and affected plants thus experience reduced tuberization [4]. Significant disease spread can therefore result in drastically reduced yield of cassava root, the starchy, edible part of the plant.

Bemisia tabaci Gennadius are commonly referred to as whiteflies due to the bright white shade of their wings. Whiteflies are vectors for ACMD and if a whitefly is carrying ACMD, it may inject the virus into the plant while feeding [5]. Additionally, female whiteflies may deposit up to 300 eggs into the mesophyll of the plant leaves. As the site of development of the eggs, the cassava plant plays a vital role in the lifecycle of this pest. Without plants on which to feed and lay eggs, the whiteflies cannot survive. Whiteflies have two different flight patterns. Short distance flights are less than 15 feet in diameter and are generally shaped like a loop. Long distance flights, in which the insects passively drift in air currents, are dependent on wind and can carry the insect significant distances depending on the properties of the air currents [6]. Adult whiteflies have limited ability to direct their flight [7] but will choose to stay on or leave a plant host based on its suitability for feeding and breeding [6]. Movement of the insects and the disease they carry is thus highly dependent on the wind.

So what is being done to solve one of African agricultures biggest problems? Several different approaches have already been analyzed in attempts to hinder the spread of this virulent virus. Phytosanitation is defined as the use of virus-free stem cuttings as planting material matched with the removal, or roguing, of infected plants from within the field. This approach focuses on systematically removing infected plant material [8]. But infected plants do not always display clear symptoms and diseased material can be introduced into new areas through the use of infected cuttings [3]. The existence of ACMD resistant varieties of cassava has been a major breakthrough in the development of strategies to combat this disease. The known resistant varieties show lower rates of ACMD, develop inconspicuous symptoms, and exhibit infection that is generally less completely systematic than in more susceptible plants [3]. Previous mathematical analysis on ACMD has often relied on geostatistics to make sense of field experiments and explain the spatial spread of the whitefly vector [9, 10]. Such analysis relies on the extrapolation of collected data and has shown that the spatial dynamics of ACMD and other such diseases are influenced by wind patterns. Additionally, various plant diseases have been studied using stochastic methods. Such analysis incorporates the probabilistic nature of disease to model transmission through non-deterministic methods. [11, 12,

13, 14].

Previous studies modeling the spatiotemporal dynamics of disease have relied on partial differential equations to demonstrate diffusion. Such research focusing on disease patterns in mammals has shed light on the mathematics governing vector-transmitted epidemics and the importance of spatial dynamics in understanding and analyzing disease spread [15, 16, 17]. An application of these methods to ACMD will provide valuable insight into the spread of the whitefly vector in space. The use of a spatiotemporal model of ACMD will enable analysis on possible methods of limiting disease incidence with the ultimate goal of maximizing harvest and preventing deadly food shortages.

In section 2 we present a temporal model for ACMD from the literature. Section 3 extends the model to the spacial domain. In section 4 we describe the numerical methods used to analyze the system, as well as describing convergence issues. Section 5 contains two analyses of sensitivity, one for the temporal model and one for the extend spacial model, and compares these. Sections 6,7, 8, and 9 contain numerical experiments on ACMD control via windbreaks and alternative spacial arrangements of plantings. Section 10 summarizes the results.

2. Holt's temporal model

Holt *et al* [3] conducted a study to model the temporal dynamics of ACMD with the goal of understanding how different variables impact the kinetics of the disease. Since contact between healthy and diseased plants occurs by means of the whitefly vector, a system of four differential equations representing healthy plants, diseased plants, non-infective whiteflies, and infective whiteflies is developed to explain the progression of the disease [3]. Holt's analysis considers the effects of the susceptibility of the plant to ACMD, the extent of the use of healthy as opposed to diseased plants for cutting, and the extent of roguing of diseased plants. Other factors that are likely to effect disease dynamics such as the intensity of cropping, the rate of crop turnover, the extent of reversion, the virulence of the disease, and the dynamics of the vector population and disease transmission are included in the model. Parameters are estimated to best represent real-world transmission of ACMD [3].

In this model, X represents the number of healthy plants, Y represents the number of diseased plants, U represents the non-infective whitefly population, and V represents the infective whitefly population. The following

4

equations are defined:

$$dX/dt = rX(1 - (X + Y)/K) - dXV - gX \quad (1)$$

$$dY/dt = dXV - aY - gY \quad (2)$$

$$dU/dt = b(U + V)(1 - (U + V)/m(X + Y)) - eYU - cU \quad (3)$$

$$dV/dt = eYU - cV \quad (4)$$

Holt [3] gives parameter values reproduced in Table 1. Note that the parameter range for growth rate has been corrected from the original paper with the author's permission.

Table 1. Parameter values and ranges.

Parameter	Standard Value	Range
K, plant density	0.5 m^{-2}	0.01-1
r, growth rate	0.05 day^{-1}	0.025-0.2
a, plant loss/roguing rate	0.003 day^{-1}	0-0.033
g, harvesting rate	0.003 day^{-1}	0.002-0.04
m, maximum vector abundance	500 $plant^{-1}$	0-2500
b, maximum vector birth rate	0.2 day^{-1}	0.1-0.3
c, vector mortality	0.12% day^{-1}	0.06-0.18
d, infection rate	0.008 $vector^{-1}day^{-1}$	0.002-0.32
e, acquisition rate	0.008 $vector^{-1}day^{-1}$	0.002-0.0032

Setting all equations equal to zero and solving for the equilibrium yields the following values :

$$X_{equ} = 0.07557 \quad (5)$$

$$Y_{equ} = 0.30382 \quad (6)$$

$$U_{equ} = 74.434 \quad (7)$$

$$V_{equ} = 1.5076 \quad (8)$$

Initial conditions for all variables in the spatiotemporal simulations are set near these equilibrium values.

3. A spatiotemporal model

The system of ordinary differential equations, in equations 1 to 4, represents the temporal dynamics of the disease. In actuality, however, the perpetuation of ACMD is highly dependent on spatial variables. Thus, we use Holt's ODE model as a basis and modify it to incorporate the spatial dynamics of the spread of the disease.

The whitefly vector should be equally likely to fly in any direction. This movement, the characteristic short distance flight patterns of whiteflies, can be represented mathematically by diffusion.

Cassava plants are stationary objects that do not diffuse. Only the whiteflies carrying the disease can be thought of as diffusing bodies. Assuming that diffusion along the z-axis, or depth-wise in space, will not affect disease transmission, we incorporate only North-South diffusion along the y-axis and East-West diffusion along the x-axis.

Applying diffusion to the model, we modify equations 3 and 4 to include the Laplacians of U and V. In accordance with the principals of diffusion, the equations for the infective and non-infective whitefly populations can be expressed as follows, where the $c_{i,j}$ s represent the diffusion coefficients specific to whitefly type (infective or non-infective) and direction (along the x axis or the y axis).

$$U_t = b(U + V)(1 - (U + V)/m(X + Y)) - eYU - cU + c_{11}U_{xx} + c_{12}U_{yy} \quad (9)$$

$$dV/dt = eYU - cV + c_{21}V_{xx} + c_{22}V_{yy} \quad (10)$$

The movement patterns of the whitefly are also highly affected by wind. These tiny insects cannot fly long distances when depending solely on their own power. But, the wind can transport a whitefly much farther than it would normally travel on its own in a short period of time. In the cassava fields in Ivory Coast studied by Lecoustre *et al* [9] and Fargette *et al* [18], there is a prevailing southwest wind. Whiteflies are thus more likely to

travel in a northeasterly direction than in any other direction. This process of being transported by wind can be modeled using advection, where the $a_{i,j}$ s represent the advection coefficients specific to whitefly type (infective or non-infective) and direction (along the x axis or the y axis).

Combining these two processes in an advection-diffusion equation yields the following equations:

$$U_t = b(U + V) \frac{(1 - (U + V))}{m(X + Y)} - eYU - cU + c_{11}U_{xx} + c_{12}U_{yy} + a_{11}U_x + a_{12}U_y \quad (11)$$

$$dV/dt = eYU - cV + c_{21}V_{xx} + c_{22}V_{yy} + a_{21}V_x + a_{22}V_y \quad (12)$$

Diffusion now represents the short distance flight of the whiteflies in all directions and advection represents the long and short distance flights of the whiteflies as influenced by wind direction and strength. Equations 1 and 2, which represent the healthy and unhealthy plant populations, remain unchanged.

4. Numerical methods

We apply the finite difference method to solve and analyze this system of partial differential equations in MATLAB. Let G be a 50x50 numerical grid to represent the plane in space where the cassava field is located.

For each entry in G, there can, theoretically, be movement to any other point on the grid. Thus, our diffusion and advection matrices must have n=2304 entries in each row to represent the 2304 non-zero entries in grid G; so, the diffusion and advection matrices are both of the size 2304 x 2304. MATLAB has a function, “delsq(G)”, which constructs the finite difference Laplacian on grid G and forms the diffusion matrix.

Mathematically, this diffusive activity is expressed by the following equation:

$$U_{xx} + U_{yy} = (u_{i+1,j} - 2u_{i,j} + u_{i-1,j} + u_{i,j+1} - 2u_{i,j} + u_{i,j-1})h^{-2} \quad (13)$$

where the error is of the order of h^2 . [19]

Using the same grid, G, as above, we construct the advection matrix, C, which is stored in MATLAB as a sparse matrix. Discrete advection is expressed by the following equation:

$$U_x + U_y = (u_{i-1,j} - u_{i+1,j} + u_{i,j-1} - u_{i,j+1})(2h)^{-1} \quad (14)$$

In this approximation, the error is of the order of $2h$ [19].

In the field, wind does not blow equally in all four cardinal directions. Wind also does not have the same velocity in all locations within the field. A southwestern wind pattern predominates in the cassava fields studied by Fargette *et al* [18] in Ivory Coast and the advection matrix must be weighted to represent differing wind velocities.

A coefficient column, referred to as *adx* in the MATLAB code, represents the vector that dictates advection in the x direction. Similarly, the vector *ady* represents the wind velocity in the y direction. Each entry in the advection matrix is weighted by its corresponding entry in these column vectors; *adx* represents the relative velocity of the wind along the x axis, but when it is paired with *ady*, which represents the relative velocity of the wind along the y axis, a 2 dimensional vector field of wind velocity in the 2-dimensional cassava field is created.

In the standard MATLAB code created for analysis, higher values are given to those entries in *adx* and *ady* that correspond to the southern and western edges because these areas are most exposed to the wind. Lower values are given to the parts of the field that are more shielded from the wind, such as the middle and the northeastern sections. This assumption stems from the field data collected by Fargette *et al*. They found that the highest concentration of whiteflies occurred in the southwestern sections of the fields due to an upwind edge effect that indicates higher levels of flight activity along the upwind edges. This increased flight activity is here attributed to greater wind velocity. [18] Thus, we use a model in which wind strength decreases as we move from south to north and from west to east.

Wind and diffusion move the whiteflies among the cassava plants within the field, but they also bring new whiteflies into the field. To model the movement of insects into the field, we add a source term to the partial differential equations so that at each time-step, a small amount of whiteflies, both infective and noninfective, are entering the field from the southwest.

The creation of grid *G*, with zeros along the boundary, facilitates the implementation of the finite difference method. However, the methods described above allow for whiteflies to be moved only among the non-zero entries of *G*. Thus, when whiteflies move beyond the numbered entries of *G* and into the boundaries due to advection or diffusion, they are lost from

the system. In real fields, when a whitefly flies outside the boundaries of a field, it may still reenter the field by flying back towards the direction from which it came. This movement is prohibited by the model and thus whiteflies enter the field only due to the source terms established in the southwest. Figure 1 shows a typical simulation.

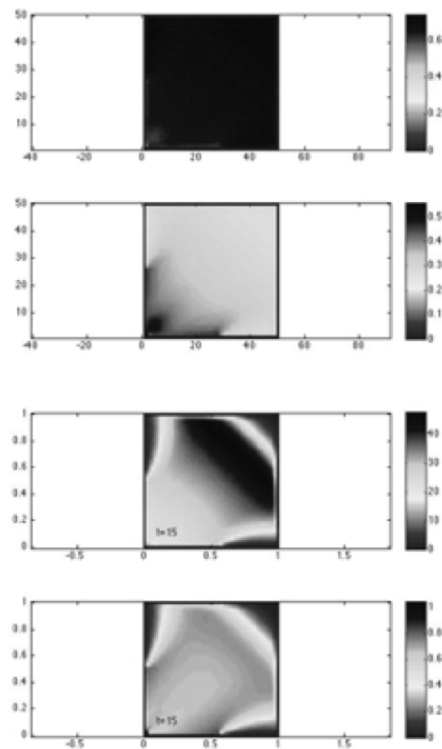


Figure 1. Simulation of the standard spatiotemporal dynamics of the ACMD system on a one-unit square with resolution of 50 by 50. a) distribution of healthy plants b) distribution of unhealthy plants c) distribution of non-infective whiteflies d) distribution of infective whiteflies

The solution calculated via the finite difference method is only an approximation of the true value of the solution of the system of equations. Further refining the grid spacing would allow for a more accurate solution; however, refinement ad infinitum is not feasible. Additionally, as the change in time between iterations, dt , tends to zero, the solution of the PDE sys-

tem should converge to the analytical solution. To evaluate the error in the approximation used for the purposes of our analysis, we evaluate how the solution changes at a particular time, $T=15$, as dt is decreased.

The original time step, dt , is 0.003; dividing this value in half. As dt is halved from 0.003 to 0.0015, the difference between the two sets of X values is on the order of 10^{-4} , as is the difference between the two sets of Y values. The error is thus less than 0.1%. The values of V and U have converged and the difference is zero. This code has very small error with respect to dt .

The grid resolution in the simulations performed in this paper is 50×50 . To test the error with respect to h , we increase this resolution and compare the results. As the grid is refined, the finite difference method solution should converge to the analytical solution. We found that scaling of $1/h^2$ applied to the source terms is needed for convergence. The difference between the values of X and Y calculated at a resolution of 50×50 and those calculated at a resolution of 100×100 is less than 0.1. The error with respect to grid spacing is greater than the error with respect to time. However, our approximations have an overall low level of error.

5. Sensitivity to parameters

Systematically changing the value of each parameter in the ordinary differential equations model by 50% of the standard value suggested by Holt *et al* and examining the effect these changes have on the ratio of healthy plants to unhealthy plants provides insight into which parameters have the greatest impact on cassava yield. Ideally, the healthy cassava population would increase as the unhealthy cassava population decreases. Maintaining a large presence of unhealthy cassava is a waste of land and resources even if it is accompanied by a large amount of healthy cassava.

Simple deduction will show that if the desired effect of any change in the system is an increase in the ratio of healthy plants to unhealthy plants, certain variables, namely r , maximum replanting rate, a , plant loss/roguing rate, and c , vector mortality should be increased by 50% while others, namely m , maximum vector abundance, b , maximum vector birth rate, d , infection rate, and e , acquisition rate, should be decreased by 50%.

A sensitivity analysis on the system of ordinary differential equations proposed by Holt *et al* shows that reducing maximum vector birth rate to 50% of its standard value has the largest positive effect on the outcome of the temporal model. Solving the ODE system with this parameter alter-

ation resulted in the highest X value and lowest Y value of all trials in which one variable was altered by 50% while all others were held constant. Second only to the effect of reducing maximum vector birth rate was the effect of increasing vector mortality to 150% of its standard value. Increasing the portion of whiteflies dying appears to have a significant positive effect on the cassava yield.

This analysis implies that the population dynamics of the whitefly are vital to the propagation of this disease in time. Model analysis predicts that controlling and limiting the vector population should lead to increased cassava yield. Experimentation with pesticides and whitefly traps are thus recommended as control method, based on the sensitivity of the temporal model.

With the goal of minimizing disease and maximizing cassava yield, we systematically alter different aspects of the spatiotemporal model and compare the results. In the standard advection diffusion program for ACMD, the total value of healthy plants, as calculated by summing the entries in the vector, X, representing health cassava plants, is 1640.5 and the total value of unhealthy plants, calculated similarly, is 745.9. Thus the ratio of healthy plants to total plants is 0.6874. Any increase in this ratio would be beneficial to the overall cassava crop, but an optimal increase in this ratio would be accompanied by an increase in total healthy cassava as this increase represents a higher yield of edible root. Under these circumstances, there would be not only a greater proportion of cassava that is healthy, but also a greater abundance of cassava in general. Therefore the food supply would increase. Unless otherwise specified, simulations have 100 time steps, corresponding to 15 time units of growth.

Performing the same parameter sensitivity analysis on the updated PDE system serves to assess the impact of adding the spatial dynamics to the system and to further examine the effects of the different parameters. All parameters were held at standard value except the one parameter under consideration in each MATLAB run. Figure 2 shows the results.

In all of the trials except the first one, in which maximum replanting rate was altered, the expected effects occur. The total number of healthy plants and the percent of plants that are healthy both increased. Increasing r , the maximum replanting rate, had a significantly negative impact on the total number of healthy plants.

Decreasing the maximum vector abundance to 50% of its standard value has only a very small impact on the abundance of both healthy and unhealthy cassava. The whitefly population remains under this maximum

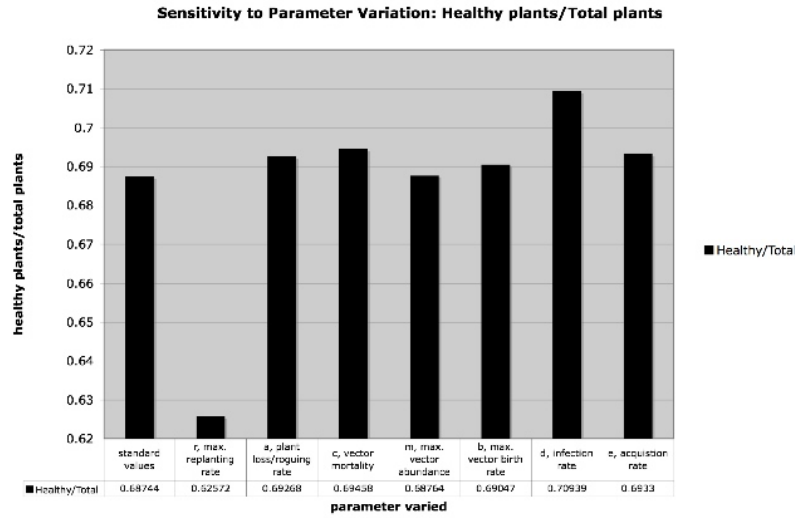


Figure 2. Sensitivity to parameter variation

abundance in the experiment and the system is therefore not affected by a change in this value so long as the maximum vector abundance is greater than the peak whitefly population.

The greatest positive impact on cassava yield occurs with a reduction in infection rate. In this scenario, the increase in total healthy plants is accompanied by a decrease in total unhealthy plants. The coupling of these two changes is the ideal result as it not only increases cassava yield from healthy plants but also decreases unhealthy plant numbers thereby reducing wasted resources and space.

Increasing vector mortality also raises cassava yield significantly. This result is concurrent with the analysis on the ordinary differential equations system. However, the parameter sensitivity analysis in the PDE system places more importance on the infection rate than does the analogous analysis performed on the ODE system. Incorporating the spatial dynamics of ACMD affects the predicted response of the disease to intervention.

6. The effects of wind

Previous work on ACMD has included observation of the distribution of disease in fields in Ivory Coast. This analysis shows an increased rate of disease incidence among plants in the southwest corner of experimental

fields. The wind-exposed borders on the south and west also showed high disease incidence and a general trend of decreasing disease with increasing distance from the southwest border. The lowest incidence was found in the middle of the field and in the northeast sections [9].

The simulations created for our analysis of the spatiotemporal dynamics of ACMD in many ways reflect these field findings. Highest disease incidence is found in the southwest corner and along the south and west borders of the simulation. Our model does display low disease rate in the center of the field; however, the lowest rate of incidence is predicted in the north, east, and northeast sections of the field as opposed to the center.

These differences may be due to differing strength of wind across the field. It is possible that the cassava plants themselves act as a sort of windbreak such that lower wind speeds are present in the center of the field. The whiteflies would be less likely to be advected into the center of the field and a lower disease incidence could thereby be observed near the middle. This wind pattern is not represented by our standard simulation.

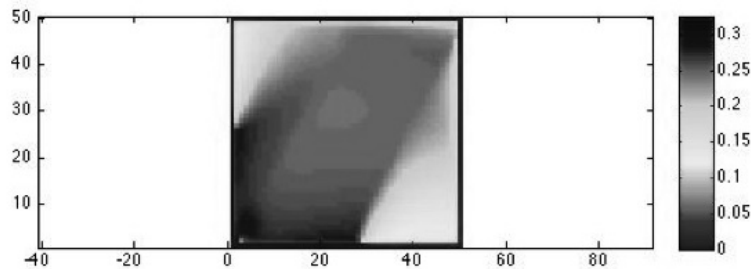


Figure 3. Simulation of the standard spatiotemporal dynamics of the unhealthy plants of the ACMD system on a one-unit square with resolution of 50 by 50 over 1000 time steps.

If our model is run for 1000 time steps instead of the 100 time steps used for most of the analysis in this paper, we see the emergence of an area in the middle of the field with lower disease incidence than the regions directly surrounding it, as shown in Figure 3. While this area fits the pattern recorded by Lecoustre *et al* [9], the lowest disease incidence in the simulation remains the corners where medium level disease incidence was observed in the field. Our model, while accurate in many regards, is not a perfect fit for this field data.

7. Whitefly “firebreaks”: some numerical experiments

With a spatial model that gives a fairly accurate representation of the collected data, we can analyze the impact of different spatial modifications on the cassava yield of the fields. We modified the spatial dynamics of the system to search for ways of increasing cassava yield and limiting disease. By creating a hole in the cassava field represented by grid G in MATLAB, we hoped to establish a trap for the whiteflies. Female whiteflies lay their eggs on the leaves of cassava plants. These leaves also serve as the main source of food for the insects; the whiteflies are thus dependent upon the cassava. By creating a section of the field that is free from plants, we hypothesize that whiteflies that reach this area will die off, unable to survive without access to cassava plants on which to feed and reproduce. Thus, there should be a reduced number of infective whiteflies, especially downwind of the plant-free plot. Because the whiteflies carry ACMD and transmit it to previously healthy plants, a reduction in whitefly population may lead to a decrease in ACMD prevalence among plants.

As predicted, this hole in the field reduces the total number of whiteflies. As the area of the plant-free square increases, the populations of both infective and non-infective whiteflies continue to decrease.

Following the removal of a 3×3 plot of cassava plants from the middle of the field, there is a 2.02% reduction in the population of infective whiteflies. Increasing the size of the plant-free area to a 5×5 square, more than doubling the plant-free area, causes a further 2.54% reduction in this population. This trend continues as the size of the cassava-free zone is increased.

As the size of the plant-free square is increased, the total healthy cassava population increases. However, the simulation with a 5×5 dead zone has only a 0.129% increase in healthy cassava, representing a rise in the percentage of total cassava that is healthy from a standard value of 67.9% to an improved 68%. While this spatial modification does increase cassava yield, it does so minimally. If the labor required to enact such a situation in a real field in Ivory Coast would be significant, then the implementation of a centered cassava-free zone would not be implicated from a cost-benefit standpoint.

The visualization of the distribution of whiteflies in a field with the above specifications illustrates a shadow effect in which the area directly northeast of the zone with no plants has a reduced whitefly population. Since whiteflies are unable to survive for any extended period of time without cassava plants, there are very few whiteflies living in the area with no

cassava. Thus, the area directly downwind of this dead zone has a very limited number of insects being advected into it and the result is the observed shadow.

To evaluate the power of this shadow in limiting disease spread to the downwind regions of the field, we reoriented the cassava-free zone and ran the program with no plants in a region closer to the southwestern borders of the field. As expected, running the MATLAB program with a 3x3 cassava free area in the southwest region of the field yields a decreased number of whiteflies, both infective and non-infective, as compared to not only the control case, but also the case with a 3x3 dead zone in the center of the field. The unhealthy plant population is also further decreased and the healthy plant population increased such that the percentage of plant material that is healthy rises to 68.1%. However, as before, this increase is quite small and the subsequent gain in cassava yield is most likely not enough to account for the added labor costs of creating this abnormal spatial distribution in planting.

We also modified the layout of the field by creating plant-free zones that divide the field into 4 smaller fields. By placing these dead zones so that the northeastern plot is the largest of the four subsections of the cassava field, we hoped to minimize the infective whitefly population and maximize healthy plants. The numerical results are in Figure 4.

As hypothesized, the subplot located in the southwest of the field has the highest concentration of infective whiteflies and of unhealthy plants. In fact, the dead zone creates such an effective barrier that relatively few whiteflies pass into the northeastern subplot and the total number of whiteflies, both infective and non-infective, is significantly reduced from the standard simulation. The total amount of unhealthy plant material is decreased and the total amount of healthy plant material is increased, raising the percentage of total healthy plants to 69.9% from an original 67.9%. Thus, total cassava yield is increased at the same time that the percentage of plant material that is healthy is increased. The coupling of these changes represents an ideal change in the dynamics of the field; an increased harvest is accompanied by a reduction in resources dedicated to the maintenance of unhealthy plants. Implementation of cassava-free zones organized in this manner is thus recommended for trial in Ivory Coast.

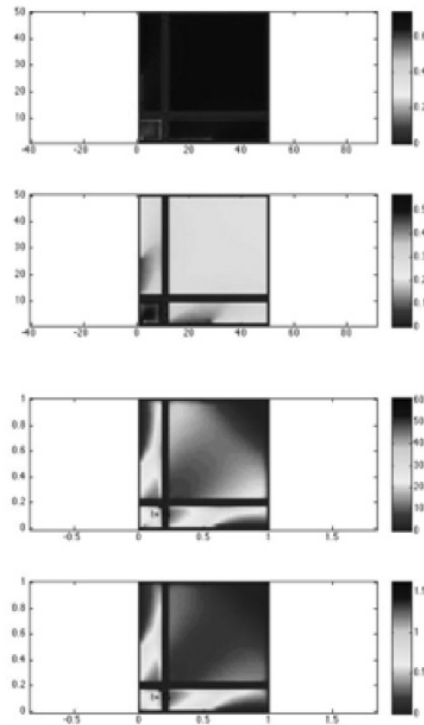


Figure 4. Simulation of the standard spatiotemporal dynamics of the unhealthy plants of the ACMD system on a one-unit square with resolution of 50 by 50 with plant-free zones dividing the field into four subfields. a) distribution of healthy plants b) distribution of unhealthy plants c) distribution of non-infective whiteflies d) distribution of infective whiteflies

8. Windbreaks: more numerical experiments

In the field, cassava growers have experimented with building windbreaks to protect against ACMD [18]. The installation of a windbreak is simulated in MATLAB by limiting the number of whiteflies that enter the field. Presumably, a windbreak does not prevent absolutely all movement of whiteflies into the field, so to represent this barrier the source terms for whiteflies are altered. The new source terms are 10% of their initial value. This demonstrates a significantly reduced, but still existent, stream of whiteflies into the field due to natural flight patterns.

This windbreak scenario yields an increase in the percentage of plants

that are healthy from the standard value of 68.7% to an improved value of 72.5%. Along with this increase, there is also an increase in the total healthy plants from 1640.2 to 1710. Thus the installation of this windbreak appears to be beneficial in that it limits the percentage of the field that is wasted due to the presence of unhealthy plants at the same time that it increases the total cassava yield. The positive effect of a windbreak is greater than the positive effect of any of the previously analyzed initiatives implying that it would be beneficial to develop real world applications of this simulation.

Next, we evaluated the dynamics of the wind. The standard model developed in section 4 assumes that wind strength decreases from south to north and from west to east due to the cassava plants themselves acting as windbreaks or buffers. What if, instead, the wind blows with constant speed at all points of the field? The wind in the area of Ivory Coast where Lecoustre *et al* [9] and Fargette *et al* [18] studied comes predominantly from the southwest, but the varying speeds within the spatial domain of the cassava fields were not recorded. The MATLAB program was altered to reflect constant wind in the southwest direction. The new value of the advection coefficient is chosen as the mid-point of the previous advection coefficient vector field. We avoid assigning wind speeds that are extremely powerful or extremely weak.

This alteration in the program yields very similar results in terms of plant population numbers as the initial program. The sum of all healthy plant material is now 1634.5 which represents 68.5% of total plants as opposed to 1640.2 plants representing 68.7% of total plants in the original simulation. This similarity is to be expected given the choice of advection constant as the median of the advection coefficient column from the earlier model. However, with constant advection, the number of non-infective flies rose to 76401 from 52791, while the infective whitefly population similarly saw a rise to 1449.9 from 1068.7. This increase in the population of the vector, especially the infective population, is not ideal and can lead to increased levels of ACMD among plants in the long run.

9. Planting density

The initial conditions for the cassava populations used in the above simulations are based on the equilibrium values of these populations as calculated from the ordinary differential equations used by Holt *et al* [3] [equations 1-4]. Clearly though, altering the equations to incorporate the spatial dy-

namics of ACMD greatly influences the outcome of the system. Therefore, we experiment with these initial conditions in hopes of discovering an ideal density for cassava planting.

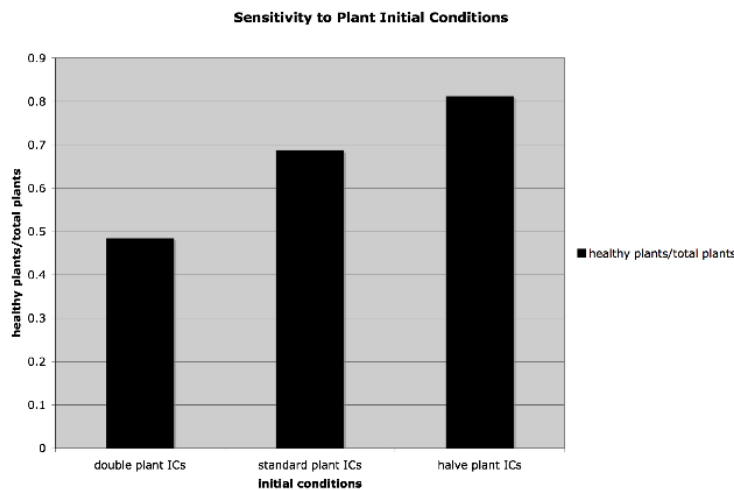


Figure 5. Sensitivity of the proportion of healthy plants to changes in the initial concentrations of healthy and unhealthy plant populations after 100 time steps in the standard simulation

Figure 5 clearly indicates that a less crowded field is beneficial to the cassava yield. Beginning the simulation with one half the number of plants, both healthy and unhealthy, results in significantly higher yield of cassava root after 100 time steps. This result may be due to the whitefly's dependence on the cassava. A reduction in cassava plants imposes a natural limitation on the whitefly population that can be sustained. With fewer total whiteflies, the vector population experiences a limited ability to spread disease among the plants and the plants therefore prosper. This rise in percentage of plants that are healthy is accompanied by an increase in the total number of healthy plants and a decrease in the total number of unhealthy plants. This ideal scenario represents a beneficial increase in cassava yield. While it may be counterintuitive for farmers to decrease the concentration of plants in their fields in order to increase the yield, this strategy is recommended for trial in fields in Ivory Coast.

10. Discussion

African Cassava Mosaic Disease causes severe food shortages throughout the African continent. A spatiotemporal model incorporating advection and diffusion based on the ordinary differential equations suggested by Holt *et al* [3] allows for the simulation of the dynamics of this disease and the vector that carries it. Systematically altering the model to represent modifications to cassava fields provides insight into the best methods of controlling ACMD and increasing harvest.

Previous analysis on parameter variation in the nonlinear interactions of the ordinary differential equations suggests that controlling the whitefly population would lead to increased cassava yield. Use of pesticides and other measures to increase vector mortality would therefore be implicated.

Similar analysis on the partial differential equations supports the data suggesting that reducing vector birth rate and increasing vector mortality would increase harvest. However, the transition from a temporal model to a spatiotemporal model fundamentally changes the system and the sensitivity analysis does not yield identical results. Such analysis on the partial differential equations suggests that reducing the infection rate would be most beneficial. Perhaps use of a naturally ACMD resistant strain of cassava could replicate this reduction in infection rate in real world applications. Such tactics are currently being employed in some cassava growing regions of Kenya [20] and Uganda. Through the National Network of cassava workers (NANEC), more than 250,000 ha of improved, resistant varieties of cassava have been planted in Uganda. The success of such programs is “explicitly illustrated by high yields of new cassava varieties that bridge the yield-gap caused by the devastating [A]CMD epidemic” [21].

The evidence that reduction in infection rate through the use of ACMD resistant varieties of cassava increases cassava yield validates the results of our simulation and further establishes the need to increase the availability and use of such strains of cassava all across Africa.

Spatial modifications relying on removal of subsections of the field appear to be minimally beneficial. The implementation of these plant-free zones are likely to create a net monetary loss because the resulting increase in cassava yield is so small that the added revenue from this additional crop may be less than the labor costs of creating the spatial modifications to the field.

However, the division of the cassava field into four unequal subfields through the elimination of all plant material in strips such that the subplot

to the southwest is the smallest and the subplot to the northeast is the largest, results in a 2.32% increase in cassava yield. We believe that this represents a significant percentage and we therefore suggest the implementation of such spatial modifications.

Significantly reducing the source term representing entry of new whiteflies into the field resulted in an increase in the percentage of total cassava that is healthy as well as an increase in total healthy plant material. The model thus suggests that preventing the entry of whiteflies into the field would increase cassava yield. Installing a windbreak along the upwind edges of the field would hopefully accomplish this trap. Experimentation with the use of windbreaks is suggested as a disease control method.

Additionally, decreasing the initial concentration of cassava in the field resulted in the greatest increase in the percentage of healthy plant material of all of the simulations used for analysis. Of course, the application of this result depends upon the field conditions currently being employed by cassava farmers, but this analysis suggests that overcrowding of the field at the beginning of the growing season can have detrimental effects on the amount of cassava harvested. Increased roguing, or the systematic removal of infected plant material, is beneficial to cassava yield; but, selective removal of all plant material, both healthy and unhealthy, also ultimately increases the amount of healthy plants.

Acknowledgments

The authors wish to acknowledge the generosity of the Neukom Institute, the National Science Foundation Epscor Program, the local chapter of the Association for Women in Mathematics and the Dartmouth Mathematics Department for supporting Zoe Lawrence to present this paper at the Society for Mathematical Biology Annual Meeting 2010.

References

1. M. Roest, <http://www.fao.org/news/story/en/item/8490/icode/>, *Food and Agriculture Organization*
2. J. P. Legg, and J.M. Thresh. Cassava mosaic virus disease in East Africa: a dynamic disease in a changing environment. *Virus Research* **71**, 135-149, (2000).
3. J. Holt, M. J. Jeger, J. M. Thresh and G. W.-Nape *J. Appl. Ecology*. **34** **3**, 793-806, (1997).
4. International Institute of Tropical Agriculture. www.iita.org. 11 Oct. 2009
5. B. James, J. Yaninek, P. Neuenschwander, A. Cudjoe, W. Modder, N. Echendu

- and M. Toko, *Pest Control in Cassava Farms*. International Institute of Tropical Agriculture. Nigeria: Wordsmithes Printers, Lagos, (2000).
6. R. F. L. Mau and J.L. Martin Kessing, Department of Entomology, Honolulu, Hawaii, http://www.extento.hawaii.edu/kbase/crop/Type/b_tabaci.htm Apr. 2007. retrieved 25 Oct. 2009.
 7. D. N. Byrne, T.B. Bellows, Jr. and M.P. Parrella. 1990. Whiteflies in agricultural systems. In: *Whiteflies: Their Bionomics, Pest Status and Management*, D. Gerling (ed.). Intercept, Hants, United Kingdom, pp. 227- 261.
 8. Thresh, J.M. and R.J. Cooter. *Plant Pathology* **54** **5**, 587-614, (2005).
 9. R. Lecoustre, D. Fargett, C. Fauquet and P. de Reffye, *Ecology and Epidemiology* **79** **9**, 913-920 (1989).
 10. D. N. Byrne, R. J. Rathman, T. V. Orum and J. C. Palumbo *Oecologia* **105** **320**, (1996).
 11. A. J. Diggle, M. U. Salam, G. J. Thomas, H. A. Yang, M. O'Connell and M. W. Sweetingham, *Phytopathology* **92** **10**, 1110-1121, (2002).
 12. G. J. Gibson *Phytopathology* **87** **2** 139, (1997)
 13. Krone, S. A Spatial model of range-dependent succession. *Journal of Applied Probability*. 37, 1044(200).
 14. B. Szymanski, T. Caraco, *Evolutionary Ecology* **8** **3**, 299-314, (1994).
 15. T. Caraco, S. Glavanakov, G. Chen, J.E. Flaherty, T.K. Ohsumi, and B.K. Szymanski, *The American Naturalist* **160** **3**, 348-359, (2002).
 16. P. Marcati and M.A. Pozio. *J. Math. Bio.* **9**, 179- 187(1980).
 17. J. D. Murray, E. A. Stanley and D. L. Brown, *Proc. R. Soc. Lond. B. Biol. Sci.* **229** **1255**, 111-150, (1986).
 18. D. Fargette, and J. C. Thouvenel, *Ann. Appl. Biol.* **106** **2**, 285-295, (1985)
 19. W. H. Press, S. A. Teukolosky, W. T. Vetterling and B. P. Flannery, *Numerical Recipes*. New York: Press Syndicate of the University of Cambridge, (1986).
 20. Kenya Agricultural Research Institute. www.kari.org. 22 May 2010.
 21. National Agricultural Research Organisation. www.naro.go.ug. 8 Oct. 2009.